RELOCATION OF EARTHQUAKES BY SOURCE-SPECIFIC STATION CORRECTIONS IN IRAN

V. Materni, A. Giuntini, S. Chiappini, R. Console and M. Chiappini

Istituto Nazionale di Geofisica e Vulcanologia, Rome, Italy

Online material: Hypocentral parameters, list of stations, events relocated and teleseimic parameters considered in this study.

Abstract

Accurate earthquake locations are crucial for investigating seismogenic processes, as well as for applications like verifying compliance to the Comprehensive Nuclear-Test-Ban Treaty (CTBT). Modeling errors of calculated travel-times may, in addition to the density of the stations, their epicentral distances and their azimuthal coverage, have the effect of shifting the computed epicenters far from the real locations, regardless of the accuracy in picking seismic phase arrivals.

In the present study, we compare the regional locations for one set of earthquakes obtained by arrival times reported by the Iranian Seismological Center (IRSC) with teleseismic locations obtained by arrival times reported by the International Seismological Center (ISC). We found location differences of the order of 10-20 km or larger, affecting both epicentral coordinates and depths. Average travel-time residuals to each station of the global network were computed for a set of sources located in the study area. We show that systematic shifts of hypocentral coordinates, as well as the sizes of their error ellipses, can be substantially reduced by applying source-specific station corrections. Finally, the validity of the calibration method was confirmed

by a test carried out on a dataset different from that used for computing the travel-time corrections.

This study includes an analysis of the effect of removing arrival times of critical stations from the dataset used for the locations, showing that this effect is largely reduced by the application of travel-time corrections.

Introduction

Since the early 1970s, evidence provided by underground nuclear explosions has shown that solutions of teleseismic location algorithms obtained using standard travel-time tables such as Jeffrey-Bullen (1940), Herrin (1968), IASPEI91 (Kennett and Engdahl, 1991), and AK135 (Kennett et al., 1995), are commonly affected by systematic errors of several km, regardless of the accuracy of arrival time picks. These errors are particularly notable for hypocenters located in complex active tectonic areas, due to the effect of strong lateral heterogeneities in those areas. Since then, further improvements in location accuracy have come from the growth of the global seismograph networks and the improvement in computing capabilities (see e.g.Veith, 1975; Chang et al., 1983; Husen and Hardebeck, 2010; Bondàr and Storchak, 2011, and references therein).

In the past years, in order to reduce the systematic errors always present in the location of seismic events, different methods have been developed. Richards-Dinger and Shearer (2000) defined empirical corrections by computing station timing corrections that continuously vary as a function of source position on a local scale. Yang et al. (2001) developed Source Specific Station Corrections (SSSCs) for regional phases and demonstrated that using SSSCs improves the quality of event location. Alternatively, on a regional scale, Myers et al. (2010) have reduced

systematic errors by replacing standard travel-time tables, based on 1-D seismic velocity models, by more sophisticated regional or global 3-D models. These models are commonly obtained by means of complex inversion algorithms using sources with accurate hypocenters, such as explosions or earthquakes with hypocenters that are well located by dense regional networks. However, the spatial resolution achievable with these methods is limited by the density of stations and the density of calibration events available in the investigated region. The validation of the results is possible through a comparison of the modeled travel-times with real observations of reference events, independent of those used in the inversion procedure.

For particular regions of high seismic activity, well covered by dense regional or local seismic networks, accurate calibration of seismic travel-times to a specific set of global stations is possible with a relatively simple method developed by Giuntini et al. (2013). They showed that mislocations of the order of 10-20 km affecting the epicenters calculated from a global seismic network in two Japanese areas can be effectively removed by using SSSCs applied to the standard travel-times. In this paper, we apply the same method to a more challenging situation, using a set of data related to a cluster of earthquakes that recently occurred in the territory of the Islamic Republic of Iran. In this case, both the number of reference earthquakes and the number of available local stations are smaller than in the case dealt with by Giuntini et al. (2013). To overcome possible systematic errors coming from the use of local/regional networks phases in the location of the reference events, in a first step of our analysis we applied the method of travel-time calibration to compute the SSSCs for the stations of the local/regional network, and relocated the reference earthquakes to be used for the computation of SSSCs at a global scale.

Information available from national seismological agencies

We have selected 17 earthquakes belonging to a seismic sequence that occurred in an area of the Iranian territory shown in Figure 1. This area is in the region of Tabriz, in the north-western part of Iran, close to the border with Azerbaijan; 17 events of magnitude between 4.1 and 6.5 (values reported by IRSC, in the Nuttli magnitude scale - Mn) which occurred in August-November 2012 were analyzed.

The earthquakes of the cluster selected for this study are not reported in the database of Ground Truth reference events maintained by ISC (see Data and Resources Section). However, locations for the events of the cluster are reported in the bulletins of the International Institute of Earthquake Engineering and Seismology (IIEES, see Data and Resources Section) and the Iranian Seismological Center (IRSC, see Data and Resources Section). As a preliminary analysis, we carried out a comparison between the hypocentral parameters reported by these two Iranian seismological agencies.

Table S1 and Table S2 (available in the electronic supplement to this article) report the hypocentral parameters together with information related to the number and geometrical distribution of the recording stations of the two networks for the earthquakes analyzed in our study. The data reported in Table S1, Table S2 and Table S3 (available in the electronic supplement to this article) testify to the higher reliability of the IRSC network data compared to the IIEES network as far as both the density of stations and their geographical distribution are concerned. In fact, in spite of the high quality of the IIEES broad-band network, the limited number of 26 stations of this network spread over the large geographical region of Iran (Ansari and Hosseini, 2014), doesn't allow the recording of more than one or two local Pg first arrivals

for a single source area, like that taken in consideration in this study. In comparison, the IRSC network includes 105 stations and is enhanced by the use of IIEES and non-national stations for locations.

Figure 2 shows a geographical comparison of the locations reported by IIEES and IRSC for the cluster of earthquakes. We can note that for this seismic sequence there is a location difference of the order of a few km for most of the events, but larger than 10 km for a few of them. In many cases the uncertainty rectangles don't overlap for the same earthquakes. There is a general trend of the IIEES locations (diamonds) to be shifted to the north with respect to those of IRSC (squares), a feature that is particularly evident for the largest epicentral differences. This trend is also shown in Figure 3 (open square in the origin of the coordinates represents the IRSC locations). Such a feature is likely due to the poorer azimuthal distribution of the IIEES stations around the epicentral area.

The uncertainties in the epicentral coordinates, represented by the thin and thick rectangles for the IIEES and IRSC locations respectively, have generally smaller sizes for the epicenters of the latter network with respect to the former.

Refinement of hypocentral parameters for events of the study area

In the previous section we noted a higher reliability of locations reported in the IRSC bulletins with respect to those reported by the IIEES, mainly in light of the higher density of stations of the network operated by the IRSC. However, we can't state that the IRSC locations are good enough to be considered ground truth events to be taken as reference for a calibration of travel-times from the source area to a network of global stations.

In order to improve our confidence in the hypocentral parameters of the selected set of earthquakes, we decided to relocate the hypocenters obtained by IRSC for the 17 earthquakes of the study area through our location algorithm for local/regional distances (using a horizontal 1-D crustal velocity model) by means of the arrival times reported in the IRSC bulletins (IRSC, see Data and Resources Section). The location algorithm is based on a straightforward least-squares iterative best-fit procedure, implemented in a FORTRAN 77 computer code. It was originally developed at the ING (Istituto Nazionale di Geofisica) in the early 1970s with the main purpose of routine processing of seismological observations from the National Seismological Network and earthquake catalog production (see, e.g., Console and Gasparini, 1976; Cagnetti and Console, 1978; Console and Favali, 1981). The very long and extensive use of this code, with some minor improvement, has demonstrated its wide applicability and robustness. In our application, only P-arrivals have been used and no quality or distance weighting has been adopted. Outliers are removed interactively by the operator.

In our relocation, we made use of 31 stations, selected with the criterion that each of them had recorded at least 13 events. The velocity model used in the location algorithm was obtained by a best-fit inversion of the IRSC travel-times computed from the origin times, arrival times and residuals reported in the IRSC bulletins (Karl F. Veith, personal communication). This model consists of a single crustal layer of Vp=6.13 km/s velocity and 48.3 km thickness overlying a Vp=8.06 km/s half space.

With the aim of limiting as far as possible the systematic shifts that could arise from a laterally non-uniform P-wave velocity in the study area, we adopted a step-by-step procedure, as described in the following.

1) From the entire database of 17 events and 31 stations, we extracted a sub-set of 7 events and 14 stations (triangles in Figure 1), with the criterion that each event was recorded by not less than 11 stations in the distance range 0-400 km, and each station had recorded a minimum of 5 events. The 7 events were located by means of the arrival times reported at these 14 stations, with a large proportion of Pg arrivals (Table S3, available in the electronic supplement to this article). The network used for this study is the result of a compromise between an optimal and a more functional configuration, aiming at fulfilling three criteria a large number of stations for the same event, a large number of events for the same station and a good azimuthal distribution of the stations.

2) The average travel-time residuals were calculated for the 14 stations and the hypocentral coordinates were computed again by means of arrival times corrected for the mean travel-time residuals. This procedure was stopped after one iteration because the last derived time residuals had not changed significantly.

3) The mean travel-time residuals of the remaining set of 17 stations (including stations at distances up to 400 km, squares in Figure 1) were estimated using the origin times and locations obtained in the previous step as reference.

4) All the 17 events of the full considered database were located by means of the arrival times at all 31 stations used, with the station corrections determined from travel-time residuals in step 2 and 3 (Table S4, locations in regular font, available in the electronic supplement to this article).

5) As a verification of locations obtained in the previous step, we have adjusted the station corrections from the travel-time residuals of the step 4 locations and finally relocated the events with these new corrections (Table S4, locations in italic font, available in the

electronic supplement to this article). The new locations converge to a stable set of station corrections and hypocentral parameters (Tables S3 and S4 available in the electronic supplement to this article and Figure 4, open diamonds).

The comparison between the IRSC locations and our new locations, shown on the map of Figure 4, illustrates differences of the order of 5 km in epicentral coordinates, but also shows a substantial similarity in their overall distribution. The comparison of their respective uncertainties highlights a reduction of the standard deviations of 51.9% and 67.5% in latitude and longitude, respectively.

The most critical parameters in hypocentral locations are depths. All depths in our locations (reported in Tables S1 and S4, available in the electronic supplement to this article) are less than 17 km. The reliability of these depth estimates is not easily demonstrable. It is generally accepted that Pg arrival times do not provide good constraint on the focal depth unless at least one of these times is from a station at an epicentral distance less than the focal depth. From Table S1 (available in the electronic supplement to this article) we can see that the closest stations used in our local/regional network locations are at epicentral distances of 22-45 km, depending on the event. However, the use of Pn together with Pg arrivals, constitutes a further constraint to depth determination. For instance, increasing the hypocentral depth from 10 to 20 km produces a delay of 0.35 s in the calculated Pg arrival time at a station of 30 km epicentral distance and a reduction of 0.9 s in the calculated Pn arrival time at a station distance of 200 km. Such variations are appreciable, given the uncertainties in phase picking for the sets of events and stations selected for this study. It must also be noted that our results are consistent with the data reported in the IRSC bulletins, which generally exhibit depths between 0 and 20 km, as typically observed in similar continental areas.

In light of the above discussion, the hypocentral coordinates and origin times obtained for the full set of 17 events (Tables S4, available in the electronic supplement to this article, locations in italics) were assumed as reasonable references for the analysis reported in the following sections.

The ISC dataset

P-wave arrival times at a selected set of seismic regional and teleseismic stations from the above mentioned earthquake sequence were obtained from the on-line ISC Bulletin (see Data and Resources Section). Figure 5 shows the global network of seismic stations used in this study and the position of the source area. The network of stations was chosen with the criterion of retaining the largest number of stations in common for all the events of the cluster.

We located the events using a least-squares single-event location algorithm developed at our Institute (INGV). The algorithm, implemented in a FORTRAN 90 code, is basically derived from that used at regional distances (described in the previous section) with the difference that in this case epicentral distances are computed from geographical coordinates through the WGS84 ellipsoid model of the Earth and travel-times are based on the IASPEI91 tables (Kennett and Engdahl, 1991). Moreover, travel-times are corrected both for the ellipticity of the Earth by the formulation of Dziewonski and Gilbert (1976), and for the station elevation. Our tests showed that these two corrections, even if they are of the order of only few tenths of second, may not be negligible in the context of our study on travel-time residuals (Carluccio et al., 2012). As in the case of the local/regional location algorithm, in these regional/teleseismic locations only first arrival times are used, without any phase quality or distance weighting.

Assuming the 17 hypocenters and origin times obtained from the procedure outlined in the previous section as a reference dataset, we computed the differences between the observed

arrival times and those computed from the reference dataset at all of the recording stations for each earthquake. For each station, we computed the average and the standard deviation of the time differences. In this exercise, we noted large residuals that exceeded twice their respective standard deviation. These arrival times were removed from the process. The final list of stations, their average distances and azimuths from the epicenters, the mean residuals and their standard deviations are reported in Table S5, available in the electronic supplement to this article.

Data analysis for the global network of stations

Here we consider the results of the analysis on the considered cluster using the data of 23 selected stations reported by the ISC (Table S5, available in the electronic supplement to this article). We used a minimum number of 17 arrival times for each of the 17 events, and each station has reported arrival times for a minimum of 14 events.

The results of the free-depth location process, using uncorrected arrival times, are shown in Figure 6. This figure shows the difference between the epicentral coordinates obtained from the global network (diamonds) and those obtained by the local/regional seismic network with the procedure described above (open square at the origin of the coordinates). We note a relevant systematic shift of about 10 km towards the north.

Figure 7 shows in a vertical cross-section the differences between the hypocentral locations obtained from the global network and those obtained by the local/regional seismic network, assumed as a reference (open square at the origin). In this figure, diamonds represent the locations without static corrections while stars represent the locations obtained adding static corrections. There is a clear systematic shift of the order of 25-30 km in the depths obtained

through the global network. Assuming that the hypocentral depths obtained from the local/regional network are not underestimated by this amount because of the constraint provided by the use of several Pg and Pn arrivals for each event, we conclude that this systematic shift is a major problem if the depth values obtained from the global network are used as a discriminant between natural and artificial sources.

We proceeded with our analysis by computing the mean residuals of the observed arrival times with respect to their expected values computed by the standard IASPEI91 travel-time tables. Several of these mean residuals, reported in Table S5 available in the electronic supplement to this article, are larger than their respective standard deviations. This observation proves that these residuals are significantly affecting the travel-times. Figure 8 shows (by the scale) the mean travel-time residuals for the stations and earthquakes considered in this study. In this figure the stations are displayed showing their average azimuth (x-axis) and distance (y-axis) from the epicenters of the reference events.

For the network of stations that recorded the earthquakes of this area, we note that there are more stations to the north than to the south. Moreover, for the northern stations, the predominance of positive time residuals (observed arrival times late relative to the calculated arrival times) at regional distances ($\Delta < 20°$) can be attributed to differences between the IASPEI91 model and the real structure of the Earth. A calculated hypocenter that is too deep will result in positive residuals at these stations. But to minimize these residuals, the location program would try to put the depth shallower.

We applied the mean residuals (reported in Table S5, available in the electronic supplement to this article) to the hypocenter location algorithm as corrections to the computed standard travel-times. The new locations obtained in this way are shown as stars in Figures 6 and 7, respectively, for the epicentral coordinates and the vertical section, relatively to the regional locations obtained by the procedure described above. The results clearly show a strong reduction of the systematic hypocenter shifts.

Figure 9 shows comparisons between the two sets of teleseismic locations and the regional reference locations. The error ellipses at a 95% confidence level for the teleseismic locations are drawn, in Figure 9a, for the locations obtained by the uncorrected arrival times (diamonds), instead are drawn in Figure 9b for the locations obtained from the arrival times corrected for the mean residuals (stars). The reference locations are represented by squares.

In Figure 9a the mislocation vectors are oriented predominantly N-S, as already evidenced by Figure 6. Only one of the reference epicenters falls outside of our error ellipse, despite the systematic mislocation of about 10 km between the two sets of epicenters. This consistency is due to the large dimensions of the error ellipses, whose semi-major axes have lengths of the order of 20 km. It is worth noting that the only event whose epicenter is strongly mislocated by 40 km to the north is the one for which the arrival time of station TORD is missing. This issue will be discussed more in detail in the following Section.

In Figure 9b we can see that the mislocation vectors have much smaller lengths, and are randomly oriented without exhibiting any systematic trend. All of our error ellipses have smaller sizes with respect to the case without corrections. Five of the 17 reference epicenters fall outside of our error ellipses, which is more than expected from statistical theory, associating a confidence level of 95% with those ellipses.

The inclusion of the mean time residuals in the location algorithm has shown the capacity to remove most of the systematic differences between the locations obtained from the global network and the reference locations obtained from the local/regional network. This performance can be quantitatively evaluated by means of a simple statistical analysis, the results of which are reported in Table 1. This table shows that the systematic bias in all the three spatial components is reduced to negligible values with respect to their statistical uncertainty by the effect of time corrections. A strong reduction is also evident for the mean horizontal shift, which is smaller than 6 km after correction. Moreover, the removal of the static residuals reduces the error ellipse areas dramatically (down to less than 20% of the original areas). The coverage (percentage of reference epicenters falling inside the error ellipses of the teleseismic locations) decreases from 94% down to 71%. This result might be related to some mislocation problems for the epicentral coordinates of the reference events.

A condition limiting the potential effectiveness of the method, especially in complex tectonic setting environments like Iran, is that station delays might not be as reliable over areas of larger geographical extension than the cluster of earthquakes of our case study.

The role of specific stations

In this Section we explore the critical role of some specific stations in the global network used for the locations. These stations are often those that fill important azimuthal gaps of the station distribution, or those that are characterized by large average time residuals.

This analysis was started by examining the consequences of removing one station at a time from the database of arrival times for all the 17 considered earthquakes. Table 2 and Table 3

report respectively, for cases without and with the application of station delays, location results obtained from the full dataset and the datasets left after removing single stations.

An interesting case concerns the removal of station AKTO, Kazakhstan. Removing this station has a much larger effect on the hypocenters and error ellipses than removing any other station, even though AKTO is not at a critical azimuth (Figure 5). This station is located to the northeast of the epicentral area, and has a mean travel-time residual of -2.2 s with the lowest residual standard deviation of all of the stations (Figure 8 and Table S5, available in the electronic supplement to this article). This negative residual is in contrast to the smaller positive values of the residuals for stations with similar azimuth, and has the effect of increasing the root mean square of the travel-time residuals and the size of the error ellipse areas. Consequently the removal of AKTO from the dataset produces an epicentral shift of several km to the southwest and a dramatic increase of the hypocentral depth, together with a substantial decrease of the average ellipse area for the 17 epicenters (compare Figures 6 and 10; Table 2). Note that the application of the travel-time corrections reduces the effects of removing station AKTO to a level more comparable to the effects of removing other stations (Table 3).

The removal of station TORD, in Africa, has the opposite effect. This station is the only one to the southwest of the epicentral area, and has a significant mean travel-time residual of -1.15 s (Figure 11 and Table S5, available in the electronic supplement to this article). Its elimination has the effect of systematically shifting the epicenters to the N (compare Figures 6 and 11; Table 2), unless also station AKTO is removed at the same time (last row in Tables 2 and 3). In fact, it can be noted that the only event whose epicenter is strongly mislocated by 40 km to the NNE with uncorrected travel-times (Figure 6) is the one for which the arrival time of station TORD is

14

missing and AKTO is included. The effect of TORD on the size of the error ellipse area is minimal, because this station primarily affects the tradeoff between the epicenter location and origin time. As with AKTO, the application of the travel-time corrections reduces the influence of the station on the hypocentral coordinates (Table 3).

The results with TORD removed clearly show that even in the case of a large gap in the azimuthal distribution (180°), the use of station corrections still reduces the shift between the teleseismic and reference locations. This reduction is critical for effective OSI to enforce the CTBT.

Testing on an independent dataset

It is well known that any hypothesis based on experimental observations must be tested by means of data that come from observations different from those that are used in the learning process. In our case, in the learning process we used the locations of a cluster of 17 earthquakes obtained by a set of 31 local/regional stations belonging to the extended IRSC seismic network and we compared the predicted arrival times with the observed arrival times observed at a global network of 23 seismic stations. In this way, we obtained travel-time corrections for our set of 23 global stations, and used them for relocating the 17 earthquakes.

In order to perform a really independent test, we collected an additional dataset composed of 10 earthquakes of magnitude Mn ranging from 4.0 to 4.3 recorded by at least 14 of the initial set of 31 local/regional stations. The hypocentral parameters for these 10 events are reported in Table S6 (available in the electronic supplement to this article). These events had not been used in the learning phase of this study, because they had not met the criterion of being recorded by a

relatively large fraction of the selected 23 stations of the global network. In fact, the number of global stations used for the teleseismic earthquake location algorithm (after having removed some clearly identified outliers) is ranges from 7 to 19. We used the ISC P arrival times at these stations in our teleseismic location algorithm. Then we located the same earthquakes by means of the same ISC arrival times, after having corrected them by the average time corrections computed in the learning phase of this study and reported in Table S3 (available in the electronic supplement to this article).

For 5 of the 10 events, the focal depths computed by the INGV teleseismic location program relative to the sea level (or more precisely, the WGS84 ground surface) were largely negative. This is mainly due to the poor geographical distribution of the stations, which doesn't provide a robust constraint for the depth determination. In this case, we do not have the information required for a comparison of depths between the locations computed with the local/regional network and those obtained in this test. For this reason, we applied the location algorithm making use of the option of fixing them at an arbitrary value of 10 km for all the events, with the advantage of increasing the reliability of epicentral coordinates, and limited the comparison only to these coordinates. This decision is a judgment call, and is certainly debatable. However, it allows a good assessment of the results as far as the epicentral coordinates are concerned.

Figure 12 shows comparisons of the epicenters for the two sets of teleseismic locations with the regional reference locations (using station corrections, Table S3 available in the electronic supplement to this article) for the dataset analyzed in this test. The error ellipses at a 95% confidence level for the teleseismic locations are drawn in Figure 12a, for the locations obtained by the uncorrected arrival times (diamonds), and in Figure 12b for the locations obtained from the arrival times corrected for the mean residuals (stars). As in Figure 9, the reference locations

are represented by squares. In this figure we can see that the mislocation vectors for the locations obtained with the time corrections (Figure 12b) have much smaller lengths than those obtained without corrections. All of our error ellipses have smaller sizes with respect to the case without corrections.

Figure 13 shows the difference between the epicentral coordinates obtained from the global network (diamonds and stars, respectively, for the uncorrected and corrected arrival times) and those obtained by the local/regional seismic network (open square at the origin of the coordinates). In this case, unlike the previous case shown in Figure 6, for the uncorrected locations we don't note any systematic shift of the epicenters. This difference is apparently due to the more sparse network used in this test compared to the network used in the learning phase, and the different number of stations used for each earthquake (ranging from 7 to 19). However, we note that, in agreement with what was observed in the previous section, the three uncorrected locations shifted to the south by more than 10 km included the arrival times from the TORD station, while the two uncorrected locations shifted to the north by more than 10 km did not include the arrival times from that station.

The better improved results obtained from the corrected travel-times are still quite evident. Again, this performance can be quantitatively evaluated by means of a statistical analysis, the results of which are in Table 4. This table shows that:

1) The average Δx and Δy shifts are much smaller than their standard deviations both for the uncorrected and the corrected locations;

2) the average horizontal shift is reduced to less than 40% of the original value by the introduction of time corrections;

3) the application of the station corrections reduces the error ellipse areas dramatically (down to less than 33% of the original areas);

4) the coverage (percentage of reference epicenters falling inside the error ellipses of the teleseismic locations) increases from 40% to 50%.

Conclusions

The analysis carried out in this study concerns a seismic sequence that occurred in Iran in the second half of 2012 and was recorded both by the two national seismic networks (operated by IIEES and IRSC) and by the global network, for which the phase data are reported in the ISC bulletins. We relocated 17 earthquakes belonging to this seismic sequence using a step-by-step method which includes the application of travel-time corrections to 31 local/regional stations recording Pg or Pn waves as first arrivals for that sequence. This step-by-step relocation method primarily improves the relative locations of the events in the cluster. However, the reliability of their absolute locations remains based upon the accuracy in the locations of the initial set of 7 events considered in the first step of the procedure.

Then we considered the arrival times for these 17 earthquakes at a global network of 23 selected stations. We found that the locations obtained from this global network are shifted with respect to those obtained from local/regional arrival times by an average distance of 12 km in the horizontal direction and by about 27 km in depth. The application of station corrections derived from mean travel-time residuals to the standard travel-times of the IASPEI91 model removed these systematic shifts.

A notable benefit of the method is that of reducing by about 50% the linear dimensions of the error ellipses from the global network locations (Table 1). A study on the effect of the presence or absence of specific stations of the network on the locations has shown the importance of certain stations, depending on their azimuthal position in the network and their time corrections. This study was also helpful for understanding the network bias. Using the ISC network without static corrections, we showed that only 2 stations are really critical: AKTO and TORD. The study has shown that static travel-time corrections can effectively moderate the influence of those stations.

The validity of the SSSC calibration method was tested by the relocation of a set of earthquakes in the same seismic area, but different from those used in the learning phase. To do this test, we selected 10 earthquakes that could be reliably located by the local/regional IRSC network but were not used in the learning phase because they had a smaller number of arrival times available in the ISC bulletins. The application of the previously determined travel-time corrections to the ISC arrival times of this independent set of earthquakes produced a substantial reduction in the average horizontal location difference as well as in the average error ellipse area, in spite of the poor constraint given by the data to the depth determination for the 10 test events.

Data and Resources

Regional locations for the events of the cluster have been obtained from the bulletins of the International Institute of Earthquake Engineering and Seismology (IIEES, http://www.iiees.ac.ir; last accessed December 2013) and the Iranian Seismological Center (IRSC, http://irsc.ut.ac.ir/; last accessed December 2013). From the latter we also obtained the phase data.

P-wave arrival times for the earthquake sequences at regional and teleseismic stations have been obtained from the on-line ISC Bulletin (http://www.isc.ac.uk; last accessed December 2013).

The figures were made using the Generic Mapping Tools version 4.5.9 (www.soest.hawaii.edu/gmt; Wessel and Smith, 1998).

Acknowledgements

We are grateful to Karl F. Veith for his invaluable comments and suggestions in the preparation of this paper. We thank also two reviewers for constructive remarks which have significantly contributed to the improvement of our manuscript, and in particular Jim Pechmann for his careful review of the paper.

References

Ansari, A., and K. A. Hosseini (2014). Broadband Seismic Network of Iran and Increased Quality of Seismic Recordings, *Seism. Res. Lett.* **85**, 878-888.

Bondàr, I., and D. Storchak (2011). Improved location procedures at the International Seismological Centre, *Geophys. J. Int.* **186**, 1220-1244, doi: 10.1111/j.1365-246X.2011.05107.x.

Carluccio, R., A. Giuntini, V. Materni, S. Chiappini, C. Bignami, F. D'Ajello Caracciolo, A. Pignatelli, S. Stramondo, R. Console, and M. Chiappini (2012). A multidisciplinary study of the DPRK nuclear tests. *Pure Appl. Geophys.*, doi: 10.1007/s00024-012-0628-8.

Console, R., and Gasparini, C. (1976). Hypocentral parameters for the Friuli May 6th, 1976 earthquake, *Annali di Geofisica*, **29**, 3, 133-137. In Italian with abstract in English.

Cagnetti, V., and Console, R. (1978). European mean travel-time and station residuals. CNEN Internal Report, RT/AMB(78) 9.

Console, R., and P. Favali (1981). Study of the Montenegro earthquake sequence, *Bull. Seism. Soc. Am.* **71**,4,1233-1248.

Chang, A. C., R. H. Shumway, R. R. Blandford, and B. W. Barker (1983). Two methods to improve location estimates - preliminary results. *Bull. Seism. Soc. Am.* **73**, 281–295.

Dziewonski, A. M., and F. Gilbert (1976). The effect of small, aspherical perturbations on travel-times and a re-examination of the correction for ellipticity, *Geoph. J. R. Astr. Soc.* **44**, 7-17.

Giuntini, A., V. Materni, S. Chiappini, R. Carluccio, R. Console, and M. Chiappini (2013). Station travel-time calibration method improves location accuracy. *Seism. Res. Lett.* **84**, 2, 225-232, doi: 10.1785/0220120124.

Herrin, E. (1968). Seismological tables for P phases, *Bull. Seism. Soc. Amer.* **58**, 1193.

Husen, S., and J. L. Hardebeck (2010). Earthquake location accuracy. *Community Online Resource for Statistical Seismicity Analysis,*

http://www.corssa.org/articles/themeiv/husen_hardebeck/husen_hardebeck.pdf.

Jeffreys, H., and K. E. Bullen (1940). Seismological Tables, *Brit. Assoc. Adv. Sci.*, 48 pp.

Kennett, B. L. N., E. R. Engdahl (1991). Traveltimes for global earthquake location and phase identification, *Geophys, J. Int.* **105**, 429-465.

Kennett B. L. N., E. R. Engdahl, and R. Buland (1995). Constraints on seismic velocities in the Earth from traveltimes, *Geophys. J. Int.* **122**, 108-124.

Myers, S. C., M. L. Begnaud, S. Ballard, M. E. Pasyanos, W. S. Phillips, A. L. Ramirez, M. S. Antolik, K. D. Hutchenson, J. J. Dwyer, C. A. Rowe, and G. S. Wagner (2010). A crust and

upper-mantle model of Eurasia ad North Africa for Pn travel-time calculation, *Bull. Seismol. Soc. Am*. **100**, 640–656, doi: 10.1785/0120090198.

Richards-Dinger, K. R., and P. M. Shearer (2000). Earthquake locations in southern California obtained using source-specific station terms. *Journal of Geophysical Research* **105**, no B5, 10.939-10.960.

Veith, K. F. (1975). Refined hypocenters and accurate reliability estimates, *Bull. Seism. Soc. Am.* **65**, 1199-1222.

Yang, X., I. Bondar, K. McLughlin, and R. North (2001). Source Specific Station Corrections for Regional Phases at Fennoscandian Stations. *Pure appl. Geophys.* **158**, 35-57.

List of Figure Captions

Figure 1. Geographic framework of the region showing the epicentral area of the earthquakes analyzed in this study (August-November 2012). Triangles and squares indicate the seismic stations used for the event locations.

Figure 2. Comparison of the IIEES (diamonds) and IRSC (squares) locations and the respective uncertainties for the earthquakes of the study area.

Figure 3. Relative mislocation of the IIEES locations (diamonds) with respect to the IRSC locations (open square in the origin of the coordinates) for the earthquakes.

Figure 4. Epicenter map of the IRSC locations (filled diamonds) and INGV relocations (open diamonds) of the same set of 17 seismic events. The sizes of the diamonds are related to the event magnitudes.

Figure 5. Epicentral area and network of stations that recorded the earthquakes analyzed in this study.

Figure 6. Mislocations of the epicenter coordinates computed by the global network with respect to the epicenter locations obtained by the local/regional network (open square at the origin of the coordinates). Diamonds represent the locations obtained by the standard global travel-times. Stars represent the locations obtained by adding static corrections to the standard travel-times.

Figure 7. Vertical section of the mislocations of the hypocenter coordinates computed by the global network with respect to hypocenter locations obtained by the local/regional seismic network (open square). Diamonds represent the locations obtained by the standard global travel-times. Stars represent the locations obtained by adding static corrections to the standard travel-times.

Figure 8. Average azimuth and distance of the stations considered in this study for the cluster of earthquakes analyzed. The respective mean travel-time residuals are shown by the scale.

Figure 9. Comparison between the epicenters obtained by our teleseismic location algorithm and those obtained by the local/regional seismic network for the cluster of seismic events analyzed in this study. (a): locations obtained using the arrival times reported in the ISC bulletins (diamonds with error ellipses). (b): locations obtained using the arrival times corrected for the static station residuals (stars with error ellipses). The reference locations are represented by squares. The line segments are the mislocation vectors.

Figure 10. As in Figure 6, having removed station AKTO from the station dataset.

Figure 11. As in Figure 6, having removed station TORD from the station dataset.

Figure 12. As Figure 9, comparison between the epicenters obtained by our teleseismic location algorithm and those obtained by the local/regional seismic network for the test cluster of seismic events analyzed in this study.

Figure 13. As in Figure 6, mislocations of the epicenter coordinates computed by the global network with respect to the epicenter locations obtained by the local/regional network (test cluster).

Table 1 Parameters obtained from statistical analysis on the relocations of the 17 seismic events with and without time corrections

	Without Corr. ± Standard Deviation	With Corr. ± Standard Deviation
Average Δx (km)	2.79 ± 2.98	0.05 ± 3.00
Average Δy (km)	9.97 ± 9.68	0.03 ± 5.93
Average Δz (km)	26.80 ± 12.08	1.72 ± 13.41
Average horiz. shift (km)	11.71 ± 8.42	5.60 ± 3.29
Error ellipse area (km^2)	1420.03	277.53
Average Smaj (km)	24.46	10.76
Average Smin (km)	18.18	7.79
Coverage (%)	94.1	70.6

Average Smaj and Average Smin are, respectively, the average semi-major and semi-minor axes of the error ellipses; the Coverage is the percentage of reference epicenters falling inside the error ellipses of the teleseismic locations.

Table

Table 2 Parameters obtained from the location process in the case without travel-time corrections

Station	No Correction							
	Average Δx (km)	Average Δy (km)	Average Δz (km)	Average Horizontal Mislocation (km)	Average Error Ellipse Area (km²)	Standard Deviation of Error Ellipse Area (km²)	Average Azimuth of Error Ellipse Major Axis (°)	Standard Deviation of Error Ellipse - Major Axis Azimuth (°)
ALL	2.79	9.97	26.80	11.71	1420	412	84.16	5.28
No AKASG	3.06	9.15	27.69	11.19	1535	453	81.95	5.10
No AKTO	-9.43	-4.11	67.50	11.94	758	272	96.39	6.65
No ARCES	2.58	11.62	28.76	12.87	1506	428	83.66	5.06
No BRTR	0.15	-6.67	-6.64	10.93	1375	618	88.60	3.28
No BVAR	3.54	10.55	25.46	12.45	1564	459	85.53	4.34
No CMAR	2.36	11.33	27.47	13.19	1738	489	75.80	3.48
No DAVOX	3.26	10.09	26.00	11.99	1530	451	84.37	5.70
No ESDC	4.34	12.13	24.15	14.13	1429	395	86.15	5.69
No EKA	3.19	9.54	25.54	11.64	1520	439	82.27	4.91
No FINES	2.53	11.22	28.17	12.47	1518	461	83.01	4.99
No GERES	2.93	9.95	26.51	11.70	1537	435	83.63	5.64
No HHC	3.58	9.10	26.85	11.50	1508	441	81.88	5.68
No HFS	2.98	9.45	26.01	11.48	1536	449	82.68	5.20
No KSAR	3.22	9.40	27.27	11.47	1470	388	83.41	6.74
No ILAR	2.76	10.41	28.13	12.26	1402	383	85.82	7.15
No MKAR	4.51	8.93	25.63	11.66	1476	357	82.28	5.91
No MLR	1.43	10.01	22.51	11.61	1384	329	83.77	5.54
No NOA	3.39	8.33	24.27	10.80	1508	447	82.65	5.21
No SONM	3.65	9.48	26.92	11.58	1515	451	82.66	5.73

No SPITS	2.54	12.27	29.76	13.67	1484	453	83.67	4.66
No TORD	5.07	25.44	25.90	26.25	1341	458	91.87	3.92
No VRAC	2.69	10.04	27.15	11.72	1528	459	83.31	5.27
No ZALV	3.17	10.09	26.77	11.94	1519	441	84.62	5.91
NO AKTO NO TORD	-7.08	4.56	62.80	10.87	908	354	106.30	4.66

The first row labeled ALL refers to the use of the full dataset of stations and all the others to the datasets left after having removed a single station at a time.

Table

Table 3 Parameters obtained from the location process in the case with travel-time corrections

Station	Yes Correction							
	Average Δx (km)	Average Δy (km)	Average Δz (km)	Average Horizontal Mislocation (km)	Average Error Ellipse Area (km^2)	Standard Deviation of Error Ellipse Area (km^2)	Average Azimuth of Error Ellipse Major Axis (°)	Standard Deviation of Error Ellipse - Major Axis Azimuth (°)
ALL	0.05	0.03	1.72	5.60	277	139	80.92	4.08
No AKASG	0.02	0.17	1.99	5.54	274	156	79.74	3.87
No AKTO	-0.11	-0.43	2.60	5.89	334	165	90.56	7.04
No ARCES	0.06	-0.02	1.39	5.64	294	150	80.73	4.12
No BRTR	0.16	0.37	4.49	6.96	312	171	91.09	6.08
No BVAR	0.10	0.04	1.96	5.46	299	153	82.31	3.79
No CMAR	-0.03	0.03	1.51	6.67	322	161	73.67	2.32
No DAVOX	0.08	0.02	1.51	5.72	293	144	81.01	4.48
No ESDC	0.11	0.21	1.37	5.92	283	131	82.72	4.59
No EKA	0.02	0.07	1.89	5.79	291	147	79.78	4.39
No FINES	0.06	-0.09	1.69	5.31	278	149	80.03	3.76
No GERES	0.07	0.02	1.63	5.58	296	147	80.28	4.41
No HHC	0.09	0.03	1.72	5.79	279	155	78.48	4.40
No HFS	0.06	0.02	1.89	5.38	295	153	79.54	3.99
No KSAR	0.02	0.02	1.73	5.54	282	131	80.09	3.64
No ILAR	0.06	-0.02	2.18	5.76	263	111	81.35	3.23
No MKAR	0.05	0.04	1.73	5.71	284	135	79.03	4.42
No MLR	0.02	0.00	0.79	5.65	235	125	81.15	4.16
No NOA	0.06	0.03	2.04	5.28	296	154	79.52	4.02
No SONM	0.06	0.02	1.72	5.54	296	151	79.85	4.45

|								
No SPITS	0.05	0.03	2.00	6.03	285	150	80.84	3.97
No TORD	0.02	-0.13	1.64	6.43	329	170	89.04	3.09
No VRAC	0.03	0.03	1.56	5.80	287	149	80.18	4.17
No ZALV	0.12	0.03	1.70	5.63	286	148	81.11	4.56
NO AKTO NO TORD	-0.17	-0.51	2.38	7.44	426	219	102.26	4.86

The first row labeled ALL refers to the use of the full dataset of stations and all the others to the datasets left after having removed a single station at a time.

Table 4 Parameters obtained from the statistical analysis on the relocations of the 10 seismic events with and without time corrections

|	Without Corr. ± Standard Deviation	With Corr. ± Standard Deviation
Average Δx (km)	-0.37 ± 11.29	-2.06 ± 4.89
Average Δy (km)	-2.07 ± 18.07	0.25 ± 5.58
Average horiz. shift (km)	17.07 ± 11.61	6.47 ± 3.65
Error ellipse area (km^2)	977.18	323.90
Average Smaj (km)	18.67	10.33
Average Smin (km)	14.44	7.51
Coverage (%)	40	50

As in Table 1, Average Smaj and Average Smin are respectively the average semi-major and semi-minor axes of the error ellipses; the Coverage is the percentage of reference epicenters falling inside the error ellipses of the teleseismic locations.
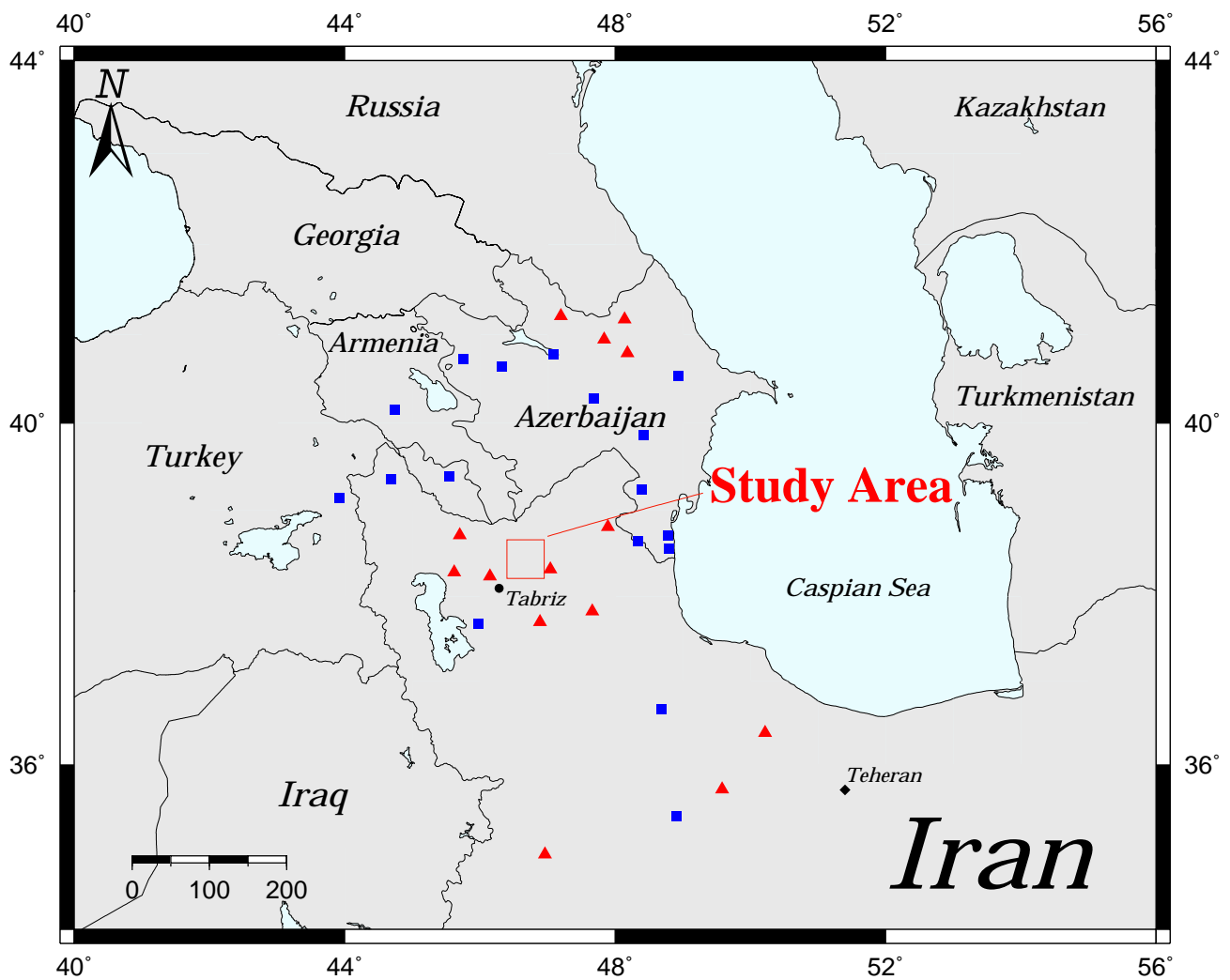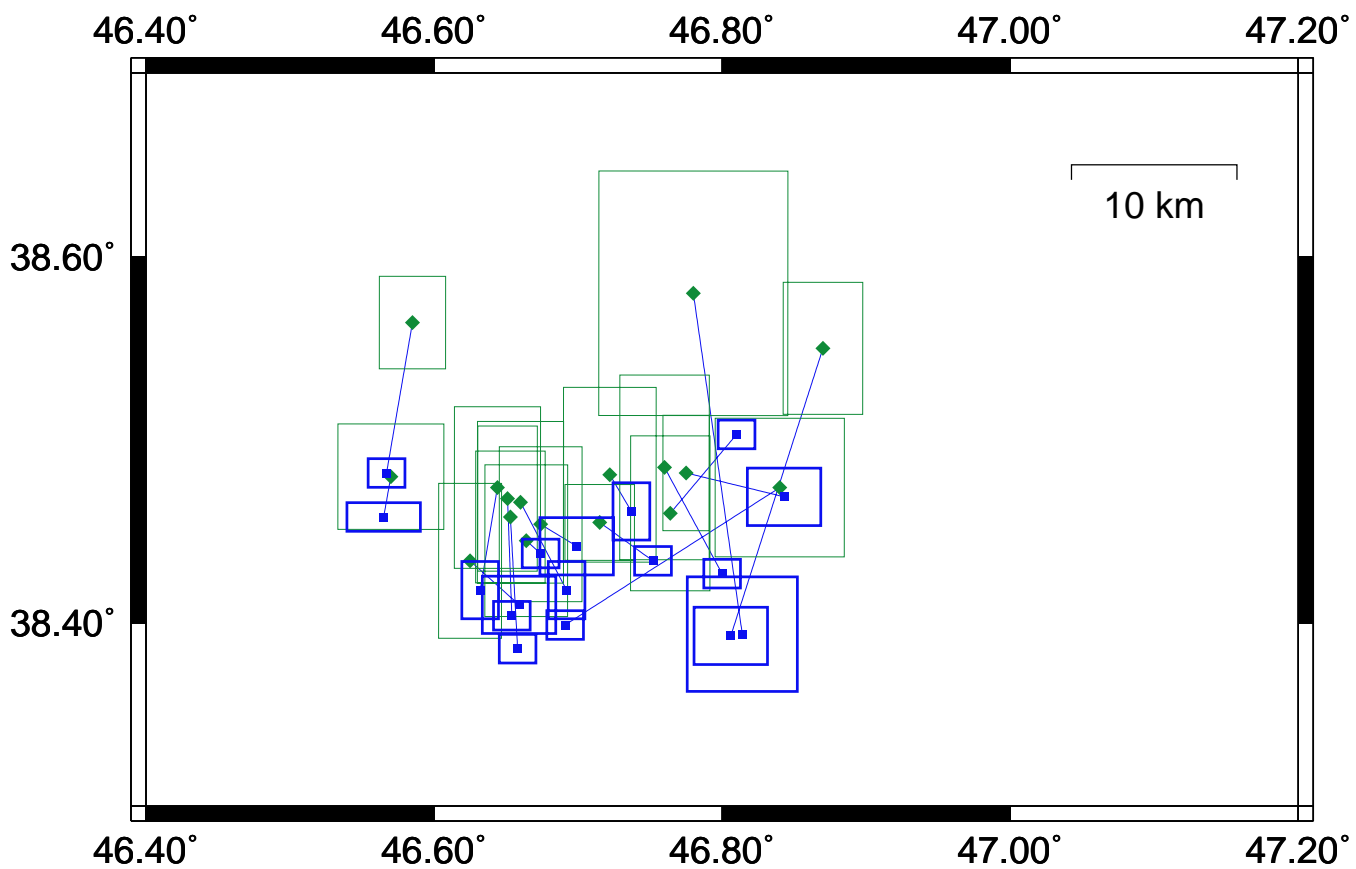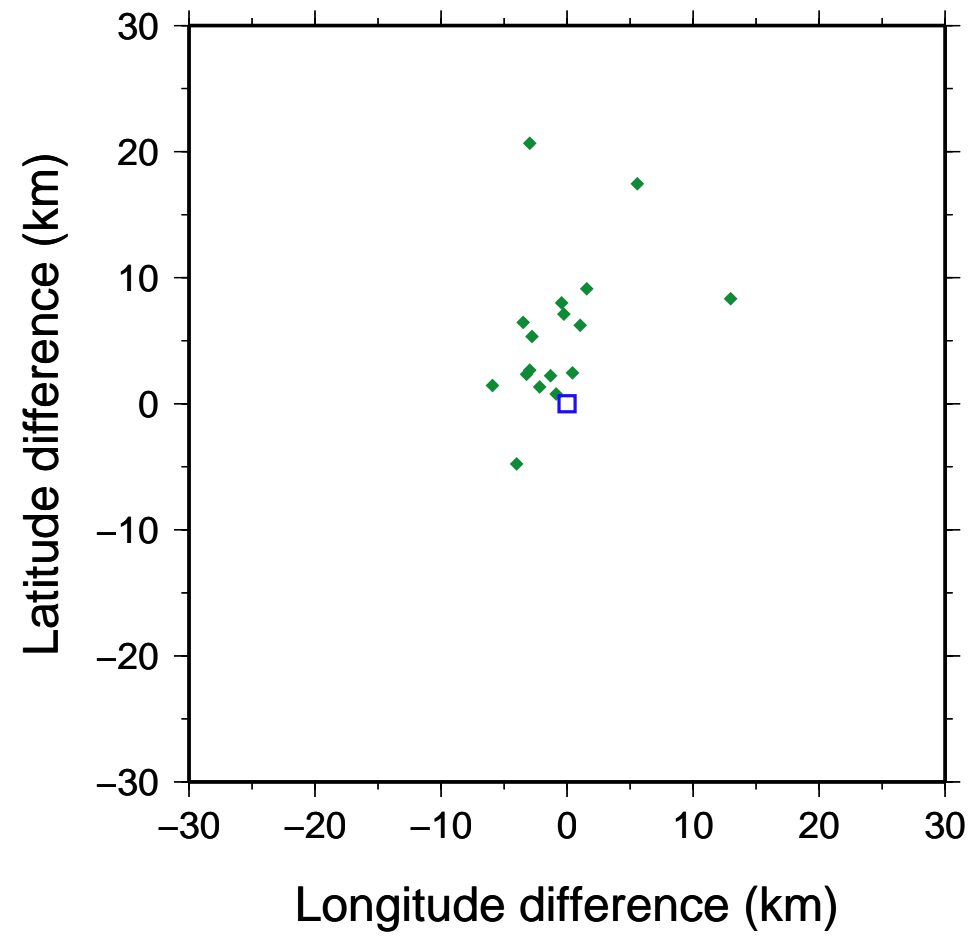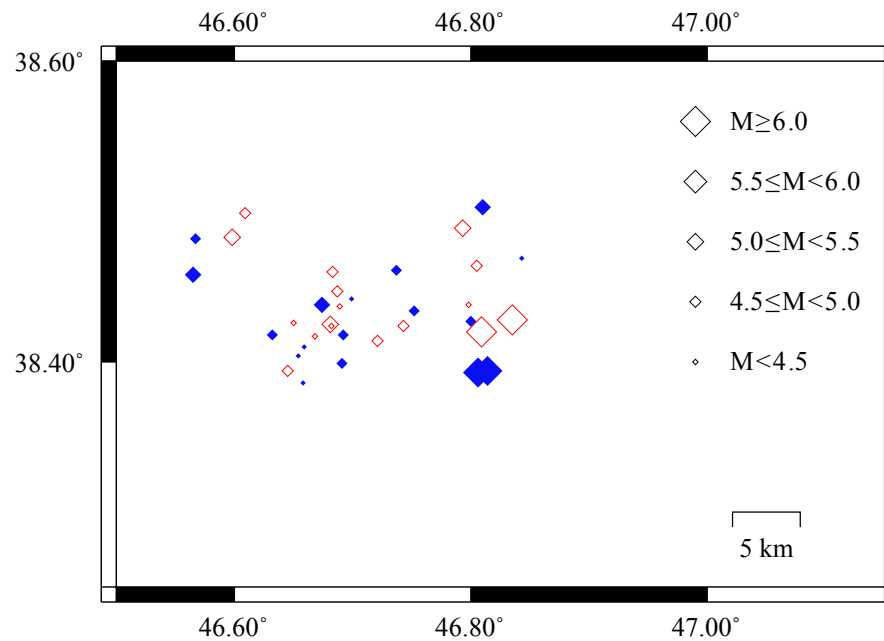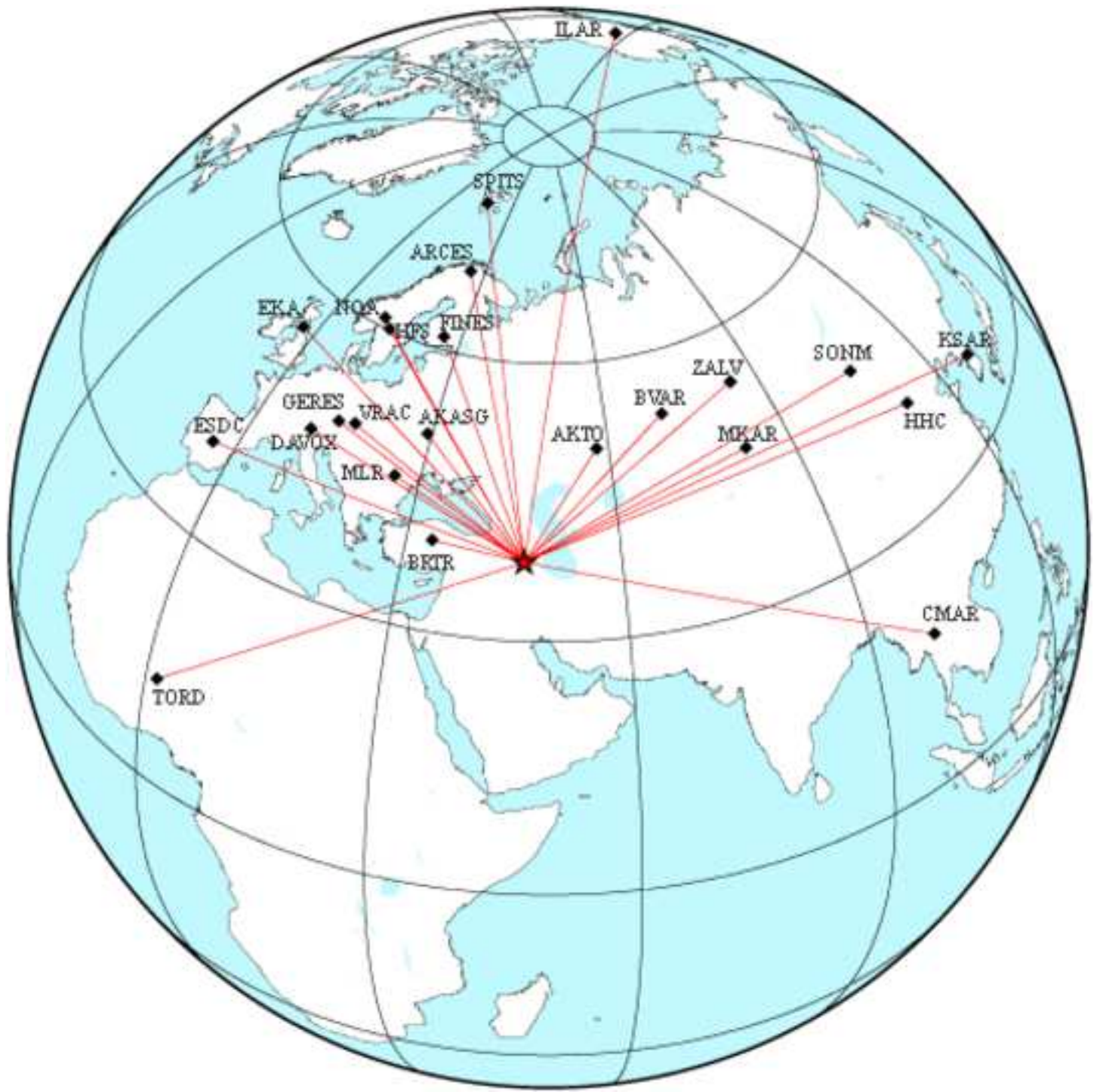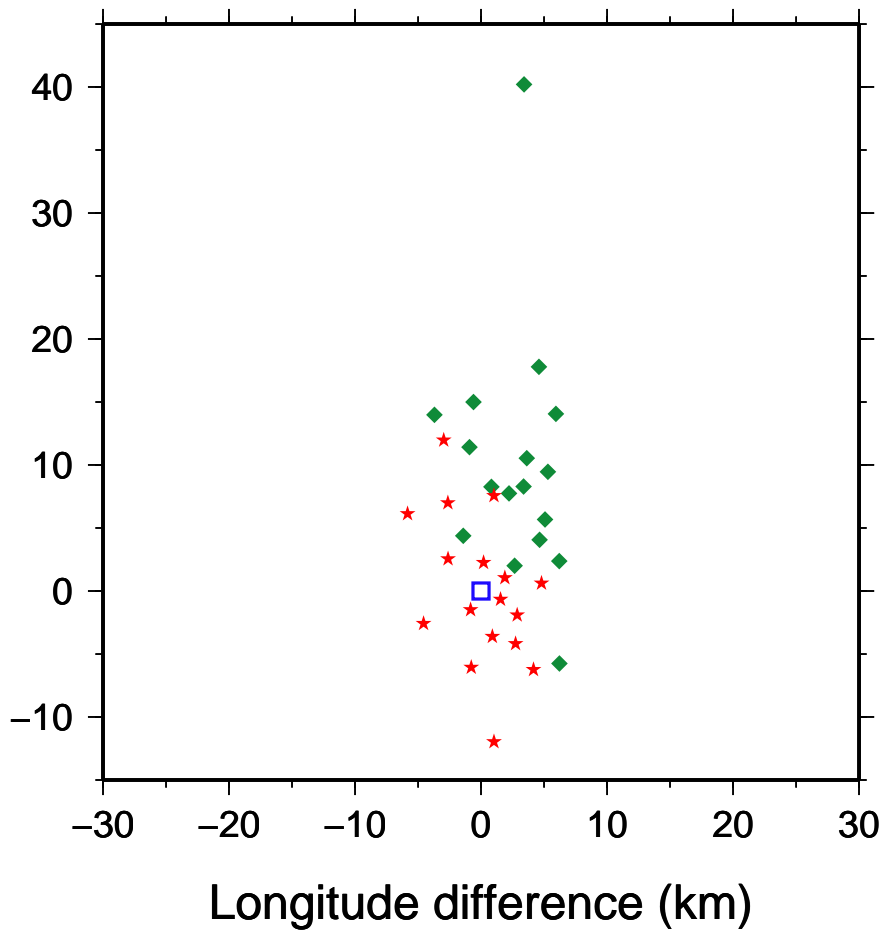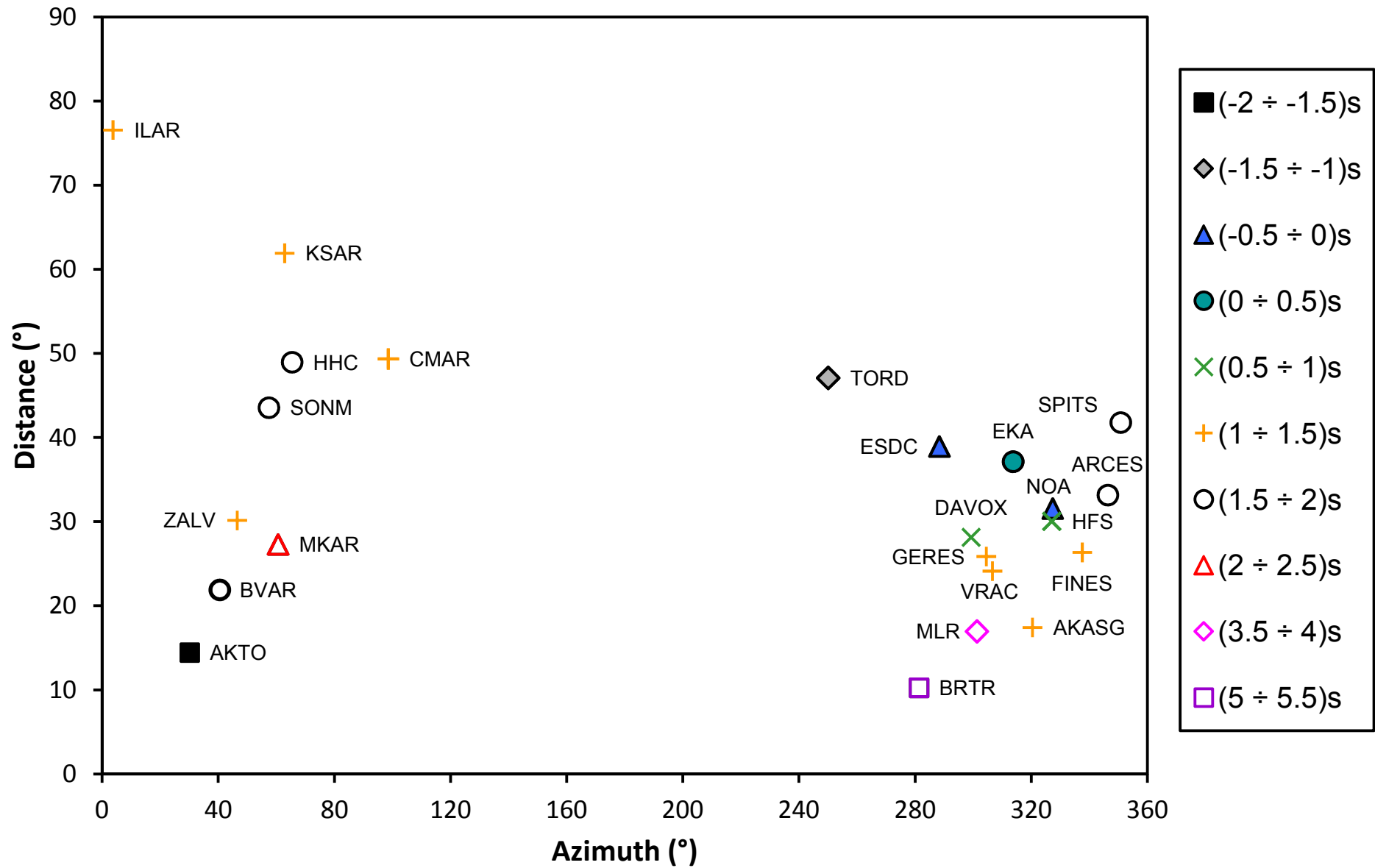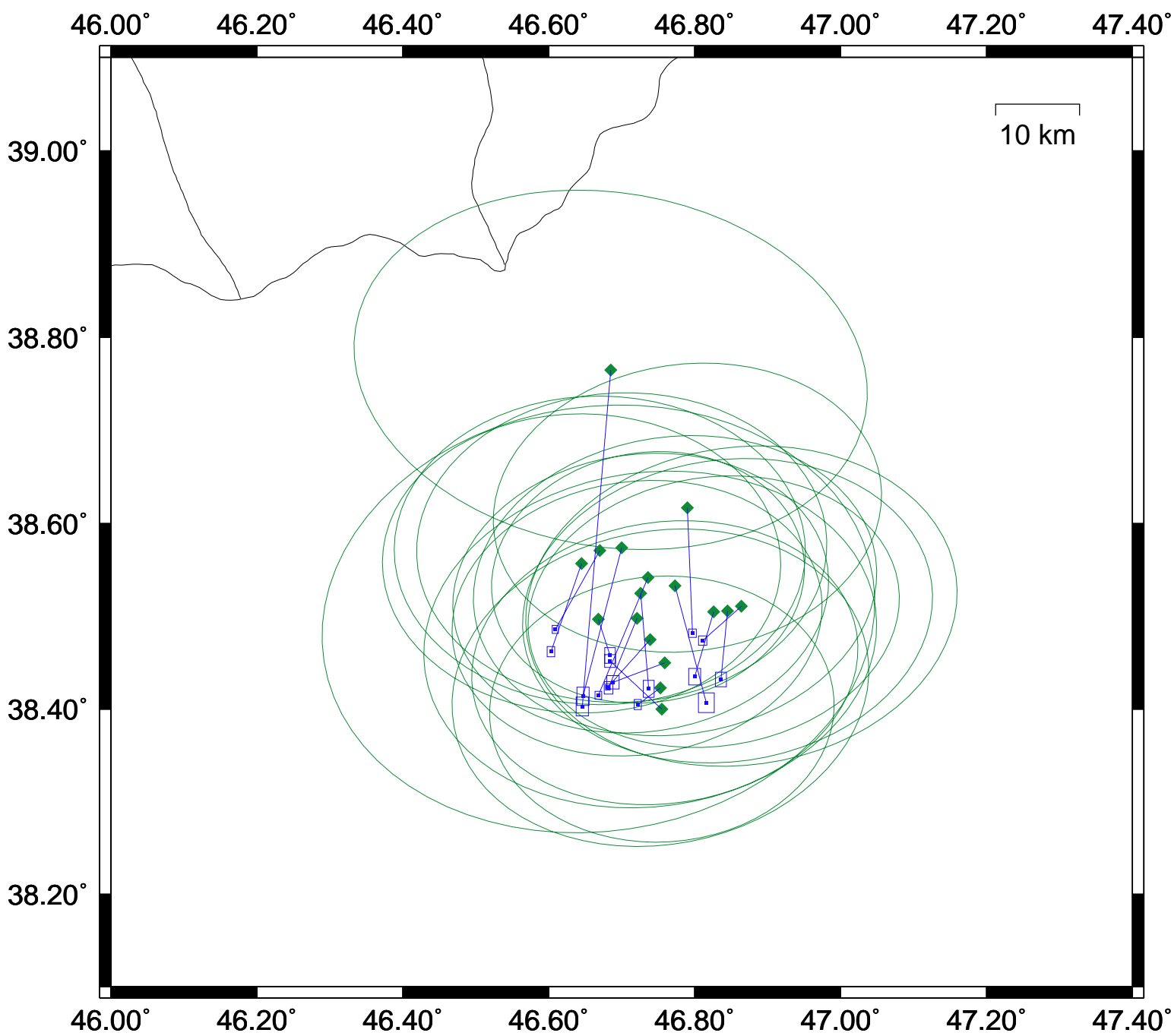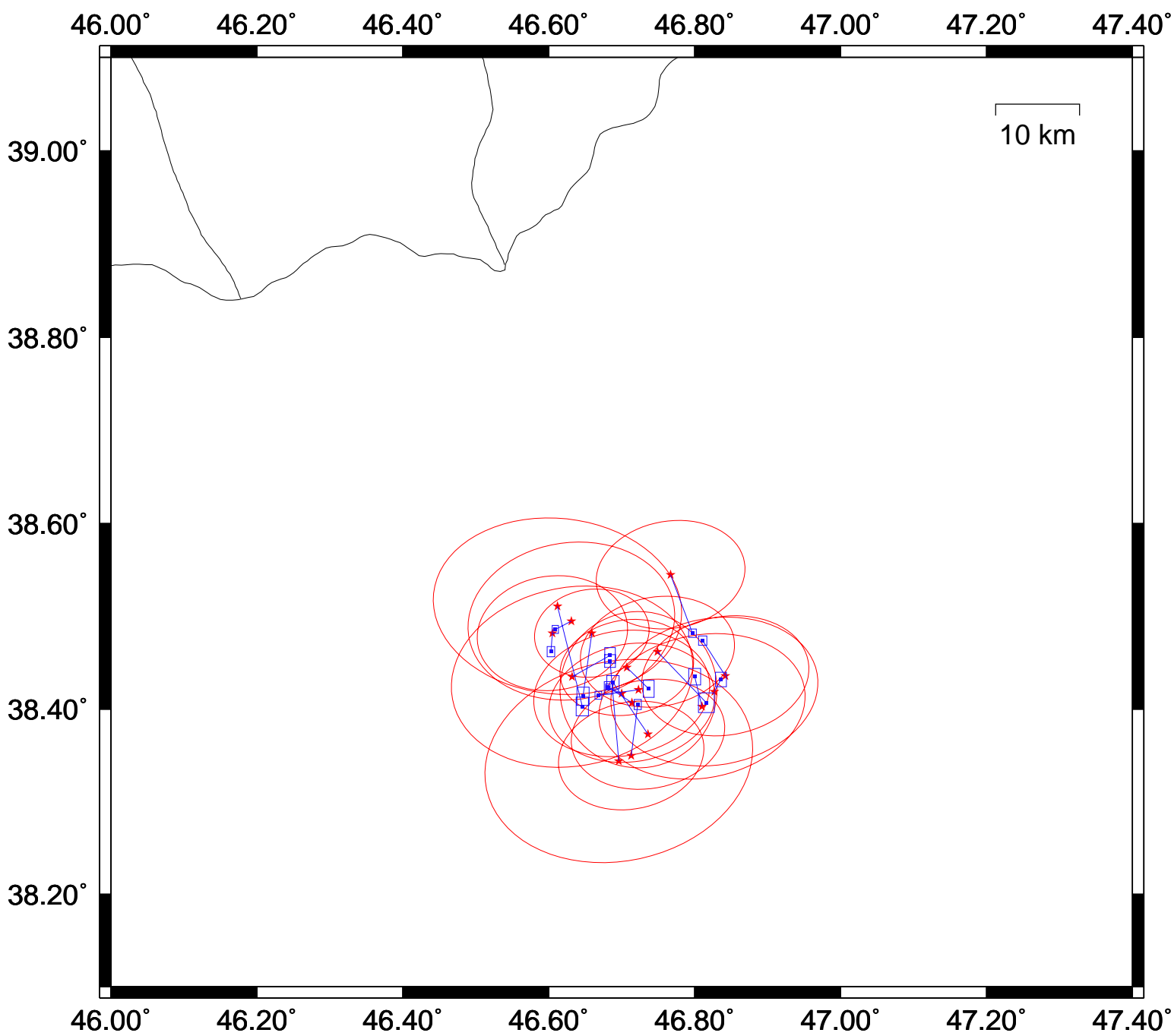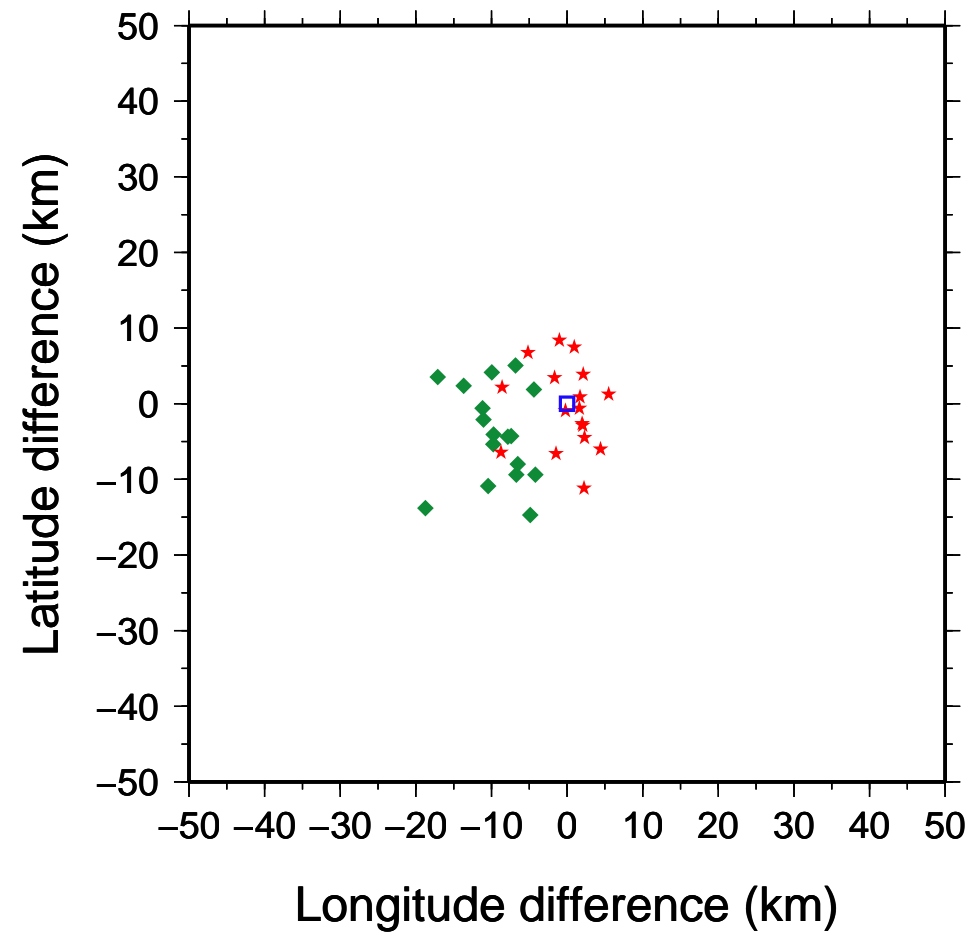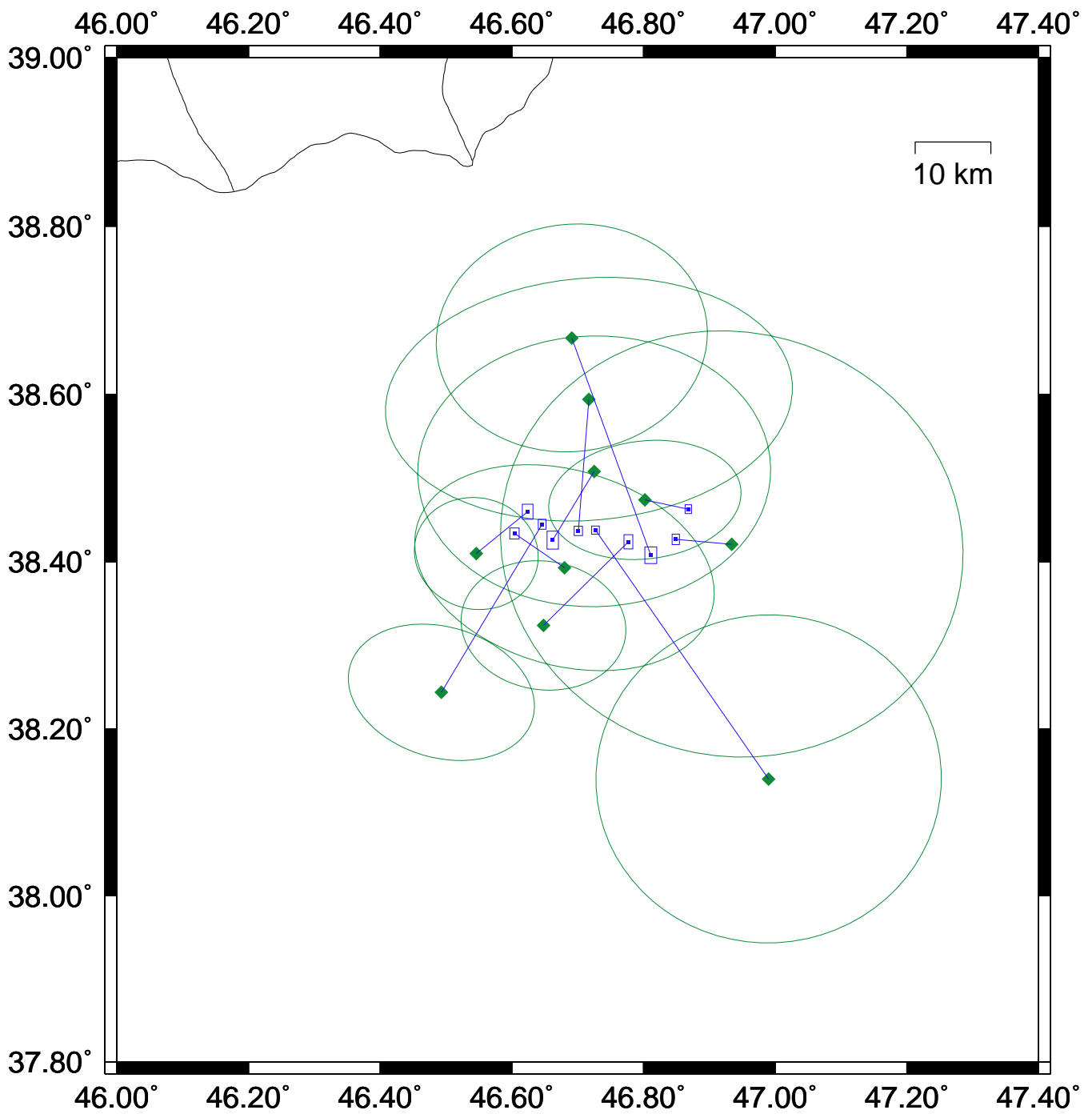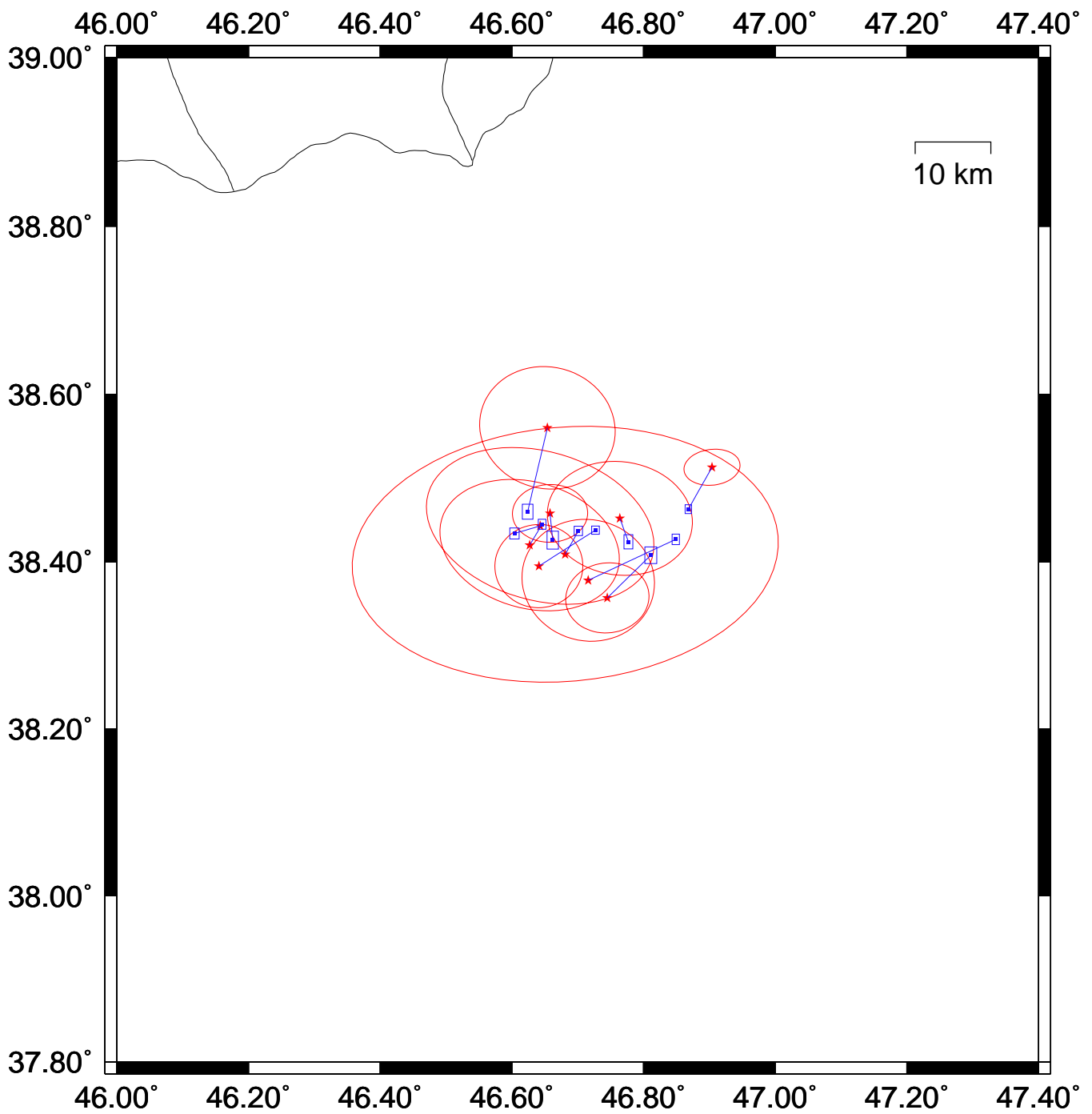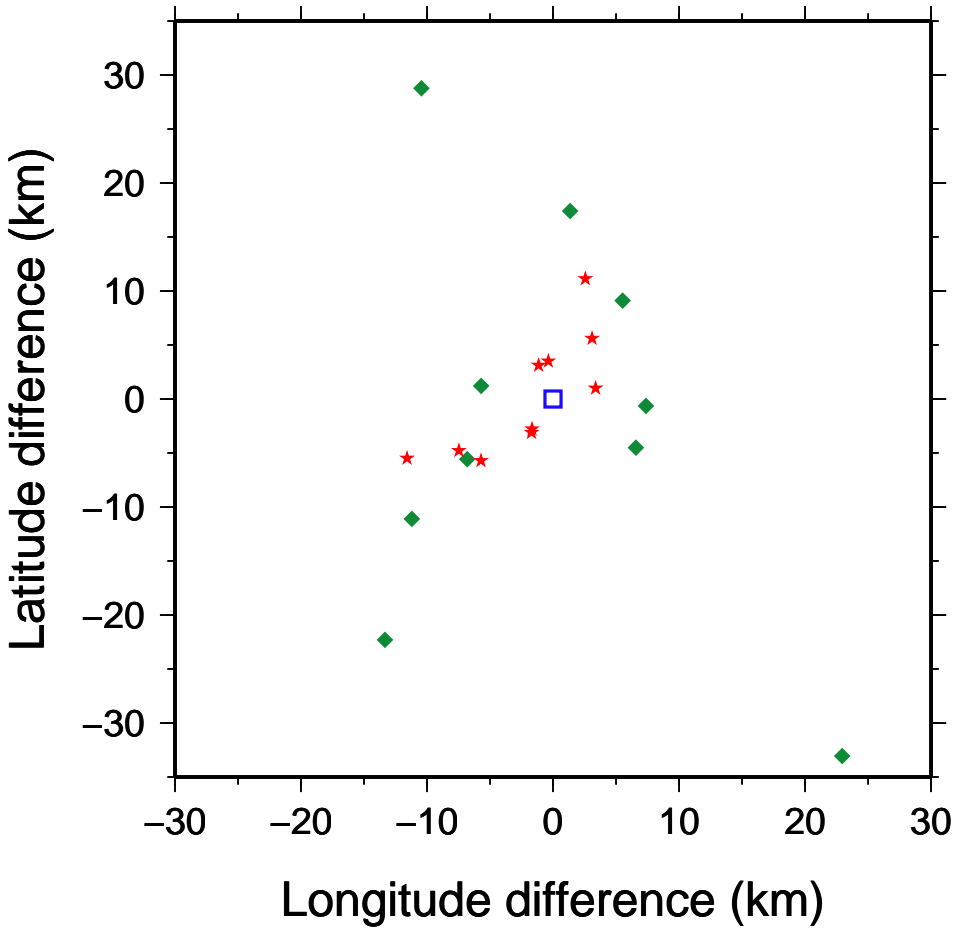
Electronic Supplement to

RELOCATION OF EARTHQUAKES BY SOURCE-SPECIFIC STATION CORRECTIONS IN IRAN

by V. Materni, A. Giuntini, S. Chiappini, R. Console and M. Chiappini

This paper contains an electronic supplement, consisting of six tables. In the Tables S1 and S2 are reported the hypocentral parameters together with information related to the number and geometrical distribution of the recording stations, respectively of the, IRSC and IIEES networks. In the Table S3 are specified the stations used for relocating the IRSC hypocenters . Table S4 reports the events relocated using arrival times corrected for the travel-time residuals at all stations. In the Table S5 are reported the parameters computed for the teleseismic analysis for each station and finally in the Table S6 are indicated the hypocentral parameters of testing cluster events.

Table S1 - The Hypocentral parameters together with information related to the number and geometrical distribution of the recording stations of the IRSC network

Event ID	Date (yyyy/mm/dd)	Time (hh:mm:ss.s)	Latitude (°)	Longitude (°)	Depth (km)	Magnitude*	RMS (s)	Azimuthal Gap (°)	Phase Arrival Times	Epicenteral Distance Range (km)
78864	2012/08/11	12:23:15.2	38.393	46.806	9.0	6.5	0.5	74	Pn, Pg (76 stations)	22-1368
62646	2012/08/11	12:34:33.8	38.394	46.184	4.0	6.3	0.8	87	Pg, Pg (61 stations)	22-1289
62647	2012/08/11	12:49:15.4	38.399	46.691	4.5	4.6	0.7	71	Pn, Pg (47 stations)	32-1209
62650	2012/08/11	13:14:05.3	38.404	46.654	8.6	4.4	0.7	69	Pn, Pg (60 stations)	35-1212
62656	2012/08/11	14:25:15.1	38.442	46.699	4.0	4.3	0.7	86	Pn, Pg (45 stations)	33-1209
70068	2012/08/11	15:21:14.5	38.427	46.800	4.0	4.7	0.7	67	Pn, Pg (76 stations)	24-1200
62662	2012/08/11	15:43:19.1	38.461	46.737	7.4	4.8	0.7	100	Pn, Pg, Sg (45 stations)	31-1205
62679	2012/08/11	19:52:44.5	38.469	46.843	4.0	4.4	0.8	93	Pn, Pg, Sg (48 stations)	24-1231
62694	2012/08/11	22:24:02.5	38.434	46.752	4.0	4.9	0.7	91	Pn, Pg, Sg (63 stations)	28-1374
62770	2012/08/12	06:40:44.6	38.386	46.658	4.0	4.1	0.7	39	Pn, Pg, Sg (54 stations)	34-981

63013	2012/08/13	01:56:10.0	38.418	46.692	4.0	4.7	0.7	91	Pn, Pg, Sg (56 stations)	33-1083
63368	2012/08/14	14:02:25.7	38.503	46.810	7.4	5.2	0.6	39	Pn, Pg, Sg (75 stations)	29-1200
63534	2012/08/15	17:49:04.6	38.438	46.674	4.0	5.0	0.5	38	Pn, Pg, Sg (60 stations)	35-1345
63982	2012/08/19	01:58:30.4	38.410	46.659	4.0	4.3	0.8	107	Pn, Pg, Sg (38 stations)	35-623
66162	2012/09/27	00:56:00.7	38.418	46.632	4.0	4.5	0.7	108	Pn, Pg (62 stations)	37-1304
68022	2012/11/07	06:26:31.2	38.458	46.565	10.0	5.4	0.8	29	Pn, Pg (77 stations)	44-1220
68689	2012/11/16	03:58:25.6	38.482	46.567	10.0	4.7	0.7	33	Pn, Pg (83 stations)	45-1312

* The magnitude of these events is computed by the Nuttli magnitude formula (Mn).

Table S2 - The Hypocentral parameters together with information related to the number and geometrical distribution of the recording stations of the IIEES network

OrigID	Date (yyyy/mm/dd)	Time (hh:mm:ss.s)	Latitude (°)	Longitude (°)	Depth (km)	Magnitude	Magnitude Type	RMS (s)	Azimuthal Gap (°)	Phase Arrival Times	Epicenteral Distance Range (km)
	2012/08/11	12:23:16.2	38.550	46.870	15.0	6.1	Mb	0.3	135	Pn, Pg, Sg (18 stations)	93-1323
	2012/08/11	12:34:35.0	38.580	46.780	16.0	6.1	Mb	0.5	134	Pn, Pg, Sg (10 stations)	99-936
1335097	2012/08/11	12:49:07.6	38.474	46.840	14.2	4.7	ML	0	158	Pn, Pg, Sg (5 stations)	99-258
1335106	2012/08/11	13:14:05.3	38.468	46.651	14.1	4.5	ML	0.1	164	Pn, Pg, Sg (3 stations)	115-268
1335173	2012/08/11	14:25:15.8	38.454	46.674	17.2	4.3	ML	0	164	Pn, Pg, Sg (3 stations)	113-266
1335181	2012/08/11	15:21:14.5	38.485	46.760	14.2	4.6	ML	0.3	131	Pn, Pg, Sg (6 stations)	105-600
1335189	2012/08/11	15:43:20.4	38.481	46.722	27.6	4.7	ML	0.2	131	Pn, Pg, Sg (6 stations)	108-601
1335464	2012/08/11	19:52:45.0	38.482	46.775	14.5	4.5	ML	0.1	160	Pn, Pg, Sg (3 stations)	104-262
1335662	2012/08/11	22:24:02.8	38.455	46.715	17.4	4.9	ML	0.2	162	Pn, Pg, Sg (3 stations)	110-264
1336151	2012/08/12	06:40:44.8	38.458	46.653	14.1	4.0	ML	0.1	164	Pn, Pg, Sg (5 stations)	115-985

1337218	2012/08/13	01:56:10.0	38.466	46.660	14.1	4.6	ML	0	164	Pn, Pg, Sg (3 stations)	114-268
1343326	2012/08/14	14:02:25.7	38.460	46.764	14.1	5.2	ML	0	160	Pn, Pg, Sg (4 stations)	106-261
1347415	2012/08/15	17:49:05.0	38.445	46.664	14.2	5.1	ML	0.1	164	Pn, Pg, Sg (4 stations)	114-468
1352487	2012/08/19	01:58:30.6	38.434	46.625	14.9	4.1	ML	0.1	166	Pn, Pg, Sg (3 stations)	118-267
1517682	2012/09/27	00:56:01.8	38.474	46.644	18.0	4.3	ML	0	163	Pn, Pg, Sg (3 stations)	115-269
	2012/11/07	06:26:30.6	38.480	46.570	14.0	5.0	ML	0.4	132	Pn, Pg, Sg (18 stations)	121-1329
1658639	2012/11/16	03:58:25.1	38.564	46.585	15.0	4.7	ML	0	161	Pn, Pg, Sg (4 stations)	117-280

Table S3 – Stations used for relocation of the IRSC hypocenters

Station	Region/State	Latitude (°)	Longitude (°)	Elevation (m)	Average Residual (s)
GZV	**Qazvin**	**36.386**	**50.218**	**2458**	**-0.674**
HRS	**Heris**	**38.318**	**47.042**	**2137**	**0.044**
IML	**Azerbaijan**	**40.793**	**48.182**	**728**	**-0.051**
LIN	**Layen**	**34.919**	**46.963**	**2140**	**0.533**
MRD	**Marand**	**38.713**	**45.702**	**2142**	**-0.037**
QBL	**Azerbaijan**	**40.946**	**47.837**	**670**	**-0.073**
SHB	**Shabestar**	**38.283**	**45.619**	**2290**	**0.209**
TBZ	**Tabriz**	**38.235**	**46.150**	**1550**	**-0.077**
QABG	**Abgarm**	**35.708**	**49.582**	**2085**	**0.100**
SEKA	**Azerbaijan**	**41.209**	**47.197**	**820**	**-0.094**
XNQ	**Azerbaijan**	**41.172**	**48.140**	**1985**	**-0.381**
BST	**Bostanabad**	**37.701**	**46.889**	**2112**	**-0.291**
SRB	**Sarab**	**37.825**	**47.663**	**1958**	**-0.157**
GRMI	**THR**	**38.810**	**47.894**	**1300**	**0.518**
LRK	Azerbaijan	38.643	48.340	1592	0.656
SAAT	Azerbaijan	39.861	48.423	13	-0.505
GLBA	Azerbaijan	39.242	48.392	140	1.493
HKZM	Koohzaman	35.378	48.905	2328	-0.235
ZRD	Azerbaijan	40.279	47.684	30	0.519
ASTR	Azerbaijan	38.560	48.791	148	0.629
GDB	Azerbaijan	40.721	45.754	1643	-0.608
CLDR	Turkiye	39.143	43.917	2087	0.506
GANJ	Azerbaijan	40.646	46.322	574	-0.784
LKRN	Azerbaijan	38.710	48.779	65	0.469
MNGR	Azerbaijan	40.773	47.085	100	0.975
SBZ	Azerbaijan	39.397	45.553	1202	0.384
GBS	Azerbaijan	40.535	48.942	827	1.246
GNI	Armenia	40.149	44.741	1583	0.763
AZR	Azar Shahr	37.678	45.984	2273	-0.017
MAKU	THR	39.355	44.683	1730	-0.744
ZNJK	THR	36.670	48.685	2200	-0.861

Bold rows indicate the 14 stations used in section "Refinement of the hypocentral parameters for events of the study area" step 1 (triangles in Figure 1), the remaining stations are used in the same section, step 3 (squares in Figure 1).

Table S4 - Events relocated by means of the arrival time at all stations corrected for the mean travel-time residuals

Date (aa/mm/dd)	Time (hh:mm:ss.ss)	Latitude (°)	Longitude (°)	Depth (km)
2012/08/11	12:23:15.53	38.432	46.836	11.66
	12:23:15.55	*38.428*	*46.835*	*11.75*
2012/08/11	12:34:34.39	38.407	46.816	5.64
	12:34:34.28	*38.420*	*46.809*	*4.54*
2012/08/11	12:49:15.51	38.452	46.684	9.34
	12:49:15.55	*38.447*	*46.687*	*9.16*
2012/08/11	13:14:05.63	38.429	46.688	8.46
	13:14:05.60	*38.437*	*46.689*	*9.95*
2012/08/11	14:25:15.72	38.423	46.682	9.36
	14:25:15.72	*38.424*	*46.682*	*9.98*
2012/08/11	15:21:14.75	38.474	46.811	13.40
	15:21:14.83	*38.464*	*46.805*	*13.36*
2012/08/11	15:43:19.87	38.405	46.722	14.13
	15:43:19.73	*38.414*	*46.721*	*15.16*
2012/08/11	19:52:44.99	38.435	46.800	11.19
	19:52:44.99	*38.438*	*46.798*	*10.95*
2012/08/11	22:24:03.01	38.422	46.737	11.01
	22:24:02.95	*38.424*	*46.743*	*13.32*
2012/08/12	06:40:44.98	38.415	46.668	9.26
	06:40:45.00	*38.417*	*46.668*	*8.28*
2012/08/13	01:56:10.21	38.458	46.684	15.62
	01:56:10.22	*38.460*	*46.683*	*15.55*
2012/08/14	14:02:26.04	38.482	46.797	15.34
	14:02:25.98	*38.489*	*46.793*	*16.69*
2012/08/15	17:49:05.17	38.424	46.681	10.62
	17:49:05.15	*38.425*	*46.681*	*11.74*
2012/08/19	01:58:30.82	38.414	46.647	10.58
	01:58:30.82	*38.426*	*46.650*	*9.45*
2012/09/27	00:56:01.00	38.403	46.646	7.69
	00:56:01.47	*38.394*	*46.645*	*6.30*
2012/11/07	06:26:30.47	38.462	46.603	11.84
	06:26:30.47	*38.483*	*46.598*	*8.90*
2012/11/16	03:58:25.18	38.486	46.609	10.55
	03:58:25.22	*38.499*	*46.609*	*6.89*

The locations in regular font are obtained with the station corrections determined from travel-time residuals (see step 2 and step 3 of section "Refinement of hypocentral parameters for events of the study area"). Then the station corrections have been adjusted with the travel-time residuals of locations in regular font and we have relocated again (italic font; see step 4 of the section "Refinement of the hypocentral parameters for events of the study area").

Table S5 - Parameters computed in the analysis for each station of the ISC network

Station	Average Epicentral Distance (°)	Average Azimuth (°)	Average Residual (s)	Residual Standard Deviation (s)
AKASG	17.427	320.39	1.084	1.134
AKTO	14.438	30.15	-2.208	0.487
ARCES	33.171	346.37	1.720	0.904
BRTR	10.247	281.34	5.165	0.820
BVAR	21.894	40.49	1.558	0.778
CMAR	49.354	98.54	1.007	0.732
DAVOX	28.152	299.26	0.811	0.689
EKA	37.142	313.73	0.324	0.503
ESDC	38.944	288.34	-0.184	0.895
FINES	26.353	337.53	1.498	1.050
GERES	25.867	304.51	1.097	0.645
HFS	30.056	327.03	0.636	0.869
HHC	48.964	65.41	1.640	1.168
ILAR	76.573	3.73	1.146	0.937
KSAR	61.920	62.84	1.266	0.561
MKAR	27.293	60.58	2.391	0.989
MLR	16.953	301.26	3.574	1.464
NOA	31.571	327.36	-0.023	0.860
SONM	43.559	57.41	1.844	0.632
SPITS	41.793	350.80	1.904	0.939
TORD	47.102	250.04	-1.151	1.048
VRAC	24.125	306.61	1.332	0.802
ZALV	30.158	46.49	1.129	0.825

Table S6 - Hypocentral parameters of the independent cluster events used in the test

Date (aa/mm/dd)	Time (hh:mm:ss.ss)	Latitude (°)	Longitude (°)	Depth (km)
2012/08/11	13:42:11.30	38.399	46.662	6.70
	13:42:11.73	*38.437*	*46.701*	*9.90*
2012/08/11	14:38:23.40	38.377	46.763	4.00
	14:38:23.52	*38.424*	*46.777*	*15.40*
2012/08/11	17:58:32.90	38.364	46.803	8.80
	17:58:33.27	*38.408*	*46.811*	*10.6*
2012/08/13	08:16:49.70	38.453	46.894	6.00
	08:16:50.16	*38.463*	*46.868*	*17.10*
2012/08/13	10:45:44.10	38.459	46.609	4.00
	10:45:44.69	*38.460*	*46.624*	*8.20*
2012/10/08	08:25:54.00	38.438	46.619	4.00
	08:25:54.58	*38.445*	*46.646*	*9.50*
2012/10/26	22:31:16.60	38.463	46.650	10.00
	22:31:16.22	*38.426*	*46.662*	*5.90*
2012/11/08	09:45:03.70	38.408	46.570	10.00
	09:45:03.29	*38.434*	*46.604*	*10.40*
2013/01/28	19:38:17.20	38.398	46.836	4.00
	19:38:17.50	*38.427*	*46.849*	*14.02*
2013/03/03	20:59:02.90	38.400	46.681	6.40
	20:59:03.21	*38.438*	*46.727*	*11.70*

The locations indicated in regular font were extracted from the IRSC bulletin, while those indicated with italics were obtained applying the station specific travel-time corrections defined in Section "Refinement of the hypocentral parameters for events of the study area" (step 4).